

When fast hydrogen atoms and negative ions are obtained from a proton beam [1] the phase volume of the beam increases because of scattering of fast particles on a gas target. In this paper, we describe a simple method of studying such scattering and report experimental data on the scattering of a beam of hydrogen atoms with energies of 5-13 keV on H₂, He, Ar, and O₂ gas targets. The study was carried out on a facility [2] containing a pulsed arc-discharge source of protons, a charge-transfer tube, a pulsed gas target, and an automated diagnostic system with a path length of 1 m, and an angular resolution of 10⁻⁴ rad. The method developed in [3, 4] for forming a proton beam from the plasma jet of an arc-discharge source, which cools during its collisionless spreading, made it possible to obtain a transverse hydrogen-atom temperature in the beam of up to several tens of millielectron-volts, and this in turn allowed the change in the transverse energy of the hydrogen atoms to be determined with an accuracy of 0.4 to 1 meV [5].

The experimental arrangement is shown in Fig. 1. The initial beam of hydrogen atoms, obtained by means of a proton charge exchange in a gas tube, is delivered to the first pair of plates 1 of a slit detector, which forms a narrow slit of width 150-500 μm and shapes a ribbon beam. The potential difference between the plates is kept at a level such that the proton component of the beam is deflected beyond the gas target 3 and the gap between the second pair of plates 4 of the slit detector used to separate the charged and neutral components of the beam. The angular spread of the beam after the gas target was measured with a multiwire secondary-emission detector (MSED) 5, placed at a distance of 1045 mm from the center of the target. The MSED has 16 gold-plated tungsten wires with a diameter of 32 μm, spaced 1.25 mm apart. The data from the MSED are processed on-line on an Élektronika-100I computer [2]. The profile, averaged over 10-30 events, and the parameters of the Gaussian curve approximating it are determined as a result of the processing. The angular spread of hydrogen atoms in the initial beam is approximated with confidence coefficient P > 0.9 by a Gaussian curve with a rms angular spread of 1.5(1 ± 0.02) · 10⁻³ to 1.65(1 ± 0.02) · 10⁻³ rad, as a function of the energy. The gas target is formed by the pulsed admission of gas through the cylindrical channel 2 into the space between the two metal electrodes forming a narrow slit of width 1 mm at the entrance and 3 mm at the exit of the target. Gas is admitted by an electromagnetic valve at a rate of 3 · 10¹⁶-3 · 10¹⁷ molecules per pulse. The thickness of the target is also varied by varying the gas accumulation in the target to the time when the beam enters it. The design used allows gas to accumulate in the region of the target in a time ≈ 400 μsec for hydrogen and ≈ 1000 μsec for argon.

The thicknesses of the gas targets are calibrated as follows. A potential difference sufficient to deflect H⁺ is established across the front pair of plates of the slit detector and a purely neutral beam is aimed at the target. A transverse clearing field of 2.5 kV/cm is formed in the region of the target; the protons produced during the charge-changing process in this field are deflected and leave the beam. The flux of neutrals traversing the target in this case is

$$I_0 = I_0^{in} \exp(-\sigma^{01}x), \quad (1)$$

where I_0^{in} is the initial H⁰ flux, x is the target thickness, and σ^{01} is the H⁰ → H⁺ stripping cross section [6-9]. By measuring the total flux of neutrals at the MSED twice, with and without the target, we can determine the target thickness. From the graphs of (I_0^{in}/I_0) as a function of T given in Fig. 2 for different targets between triggering of the pulsed electromagnetic valve and the formation of the pulsed beam we see the thickness of the gas target is proportional to the gas accumulation time. Equation (1) is suitable for calibration of both thin and thick targets, since the calibration accuracy is not limited by the

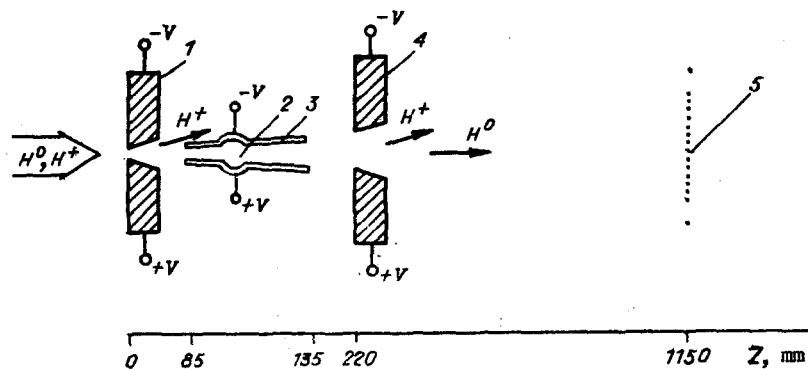


Fig. 1

process whereby charge-exchange equilibrium is established and does not decrease as the target thickness grows. In a number of cases the target thickness was also calibrated from the ratio of the H^0 and H^+ fluxes in the beam, which was established after passage through the target. The two calibration methods gave identical results.

The angular spread of particles in the beam was measured with and without a clearing field in the region of the target. The first case corresponds to scattering without charge exchange since before becoming neutrals again in another charge exchange, virtually all of the protons produced as a result of charge exchange manage to acquire sufficient transverse velocity in the clearing field to be deflected out of the aperture of the MSED. It is described by the scheme $H^0 + M \rightarrow H^0$ (M is a molecule or atom of the target). In the second case secondary neutrals formed according to the scheme



pass into the MSED. Points 1 in Fig. 3 represent the dependence of the acquired transverse energy of the beam $E_{\perp} = \alpha_t^2 E$ on \bar{x} [\bar{x} is the thickness of the Ar gas target, measured in units of $1/(\sigma^{01} + \sigma^{10})$] at a hydrogen atom energy E of 5 keV in the presence of a clearing field. The rms angle of beam scattering on the target is found from

$$\alpha_t^2 = (\sigma_t^2 - \sigma_0^2)/L^2$$

(σ_0 and σ_t are the Gaussian widths of the beam profiles without and with the target and L is the distance from the target to the MSED). As follows from Fig. 3, the acquisition of transverse energy is proportional to the thickness of the gas target, $E_{\perp} = k\bar{x}$. A similar proportionality has also been determined for other gas targets. Table 1 shows the values of k for H_2 , He, Ar, and O_2 gas targets (condition A).

The difference of the beam profiles obtained in experiments with and without a clearing field constitutes the profile of a beam of hydrogen atoms, which have intermediate

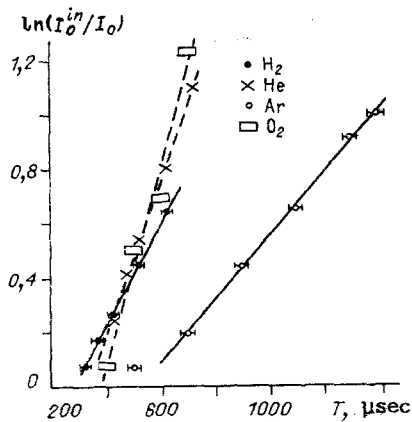


Fig. 2

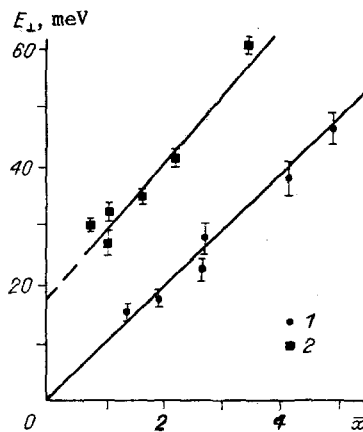


Fig. 3

TABLE 1

Target	Condi- tions	E, keV	$E_{\perp} = E_0 + kx$	
			E_0 , meV	k, meV
H ₂	A	5,2	0	4,2±0,4
	A	10,4	0	5,05±0,8
	A	13,0	0	5,9±1,0
He	A	5,0	0	7,5±1,8
	A	13,0	0	6,7±4,3
Ar	A	5,0	0	9,5±0,7
	A	11,0	0	4,8±0,4
	B	9,0	18,1±2,1	11,4±1,0
O ₂	A	11,2	0	19,2±0,9
	B	11,2	20,0±7,0	14,4±3,2

TABLE 2

Target	E, keV	Differential scattering cross section	
		A	θ_0 , mrad
Ar	11,0	0,1(1±0,09)	3,55(1±0,13)
Ar	9,0	0,36(1±0,21)	4,5(1±0,36)
H ₂	8,3	0,24(1±0,12)	4,4(1±0,22)
He	8,4	0,28(1±0,29)	5,6(1±0,22)

charged states (2) in the region of the target. The rms scattering angle for such particles is found from

$$\alpha_t^2 = (\sigma_d^2 - \sigma_0^2)/L^2$$

(σ_d is the Gaussian width of the difference profile). Points 2 in Fig. 3 represent the dependence of the acquisition of transverse energy $E_{\perp} = \alpha_t^2 E$ by a beam of 9-keV hydrogen atoms, which had undergone a double charge exchange in an Ar target, on the target thickness \bar{x} , which is satisfactorily approximated by a straight line $E_{\perp} = k\bar{x} + E_0$ (E_0 is the average value of the acquisition of transverse energy in a double charge exchange). A similar linear relation exists for other gas targets as well. The values of E_0 and k are shown in Table 1 for Ar and O₂ (condition B).

Our analysis was carried out within the framework of the simple model of small-angle scattering. At the same time large-angle scattering of an appreciable part of the beam is observed. A "pedestal" which increases with the target thickness appears in the profile of the beam that has traversed the target. As an illustration Fig. 4 shows the profile of the initial beam (1) with the Gaussian curve approximating it and the profile of the beam (2) after traversal through an Ar target with a thickness $5/(\sigma^{01} + \sigma^{10})$, at a beam energy of 11 keV. As a result of a more detailed mathematical analysis of the data (see Appendix), which were obtained in experiments with the clearing field switched on, we determined the differential scattering cross section $\sigma^{00}(\theta)$ in the range of scattering angles $10^{-3} \leq \theta \leq 10^{-2}$. The dependence $\sigma^{00}(\theta)$ was approximated by the Gaussian function

$$\sigma^{00}(\theta) \approx A \frac{\sigma^{10} + \sigma^{01}}{2\pi\theta^2} \exp(-\theta^2/2\theta_0^2).$$

The parameters A and θ_0 for the series of targets are given in Table 2.

In a number of cases, e.g., scattering on Ar at an energy $E = 9$ keV, the cross section $\sigma^{00}(\theta)$ is not described sufficiently well by the Gaussian function and as a result the parameters are determined with a large error. For detailed information about the differential scattering cross section we must increase the number of profilometer measuring channels. The results show that in processes not accompanied by charge exchange, a considerable part of the hydrogen-atom beam is scattered through angles that are much larger than the characteristic angle of $5 \cdot 10^{-4}$ of scattering [10] during a charge-changing transformation of protons to hydrogen atoms.

In summary, using beams of fast hydrogen atoms with a low transverse temperature and employing a target of original design, we have realized a simple method of studying the scattering of fast hydrogen atoms on gas targets and determined angular broadening of the beam of fast hydrogen atoms on H₂, He, Ar, and O₂ targets.

Appendix. The experimental profiles reflect the one-dimensional density distribution of the hydrogen atom flux in the plane of the MSED or, with allowance for the collimation of the beam before entry into the gas target, the one-dimensional angular distribution $J_0(\alpha)$ of the hydrogen atoms. Additional mathematical processing of the data was carried out as follows. The scale of the angles is extended so that the angular aperture of the

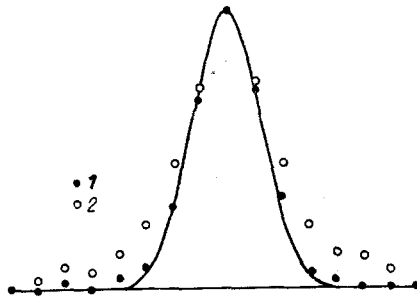


Fig. 4

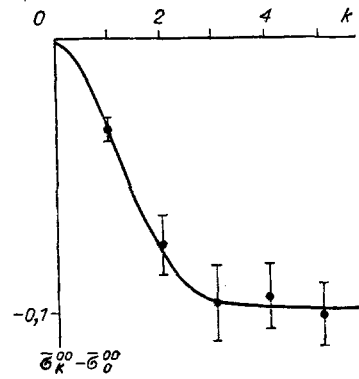


Fig. 5

MSED becomes equal to 2π and the experimental profile of the beam is replaced by a periodic function with period 2π . Provided that the beam density at the edges of the MSED aperture, such an exchange does not affect the result. The observed distribution is discretely Fourier-transformed [11]. If in this way we change the scale of the angles of one-dimensional partial differential scattering cross sections

$$\bar{\sigma}^{ij}(\theta) = \int \sigma^{ij}(\sqrt{\theta^2 + \alpha^2}) d\alpha$$

[where $\sigma^{ij}(\theta)$ is the differential scattering cross section with a transition from the i -th to the j -th charge state H^0, H^+] and expand them in a Fourier series

$$\bar{\sigma}_k^{ij} = \frac{1}{\pi} \int_{-\pi}^{\pi} \bar{\sigma}^{ij}(\varphi) \cos k\varphi d\varphi,$$

then the equations describing the variation of the angular distribution functions $J_0(\alpha)$ and $J_1(\alpha)$ of the beam particles for the neutral and charged components

$$\begin{aligned} \frac{\partial}{\partial x} J_0(\alpha) &= \int [\bar{\sigma}^{00}(\varphi)(J_0(\alpha - \varphi) - J_0(\alpha)) + \bar{\sigma}^{10}(\varphi)J_1(\alpha - \varphi) - \bar{\sigma}^{01}(\varphi)J_0(\alpha)] d\varphi, \\ \frac{\partial}{\partial x} J_1(\alpha) &= \int [\bar{\sigma}^{11}(\varphi)(J_1(\alpha - \varphi) - J_1(\alpha)) + \bar{\sigma}^{01}(\varphi)J_0(\alpha - \varphi) - \bar{\sigma}^{10}(\varphi)J_1(\alpha)] d\varphi \end{aligned}$$

are transformed into equations for the harmonics,

$$\begin{aligned} \frac{\partial}{\partial x} J_0^k &= \pi (\bar{\sigma}_k^{00} - \bar{\sigma}_0^{00}) J_0^k + \pi (\bar{\sigma}_k^{10} J_1^k - \bar{\sigma}_0^{01} J_0^k), \\ \frac{\partial}{\partial x} J_1^k &= \pi (\bar{\sigma}_k^{11} - \bar{\sigma}_0^{11}) J_1^k + \pi (\bar{\sigma}_k^{01} J_0^k - \bar{\sigma}_0^{10} J_1^k). \end{aligned} \quad (3)$$

The solution of system (3) is the sum of two components. Consequently, the problem of finding the differential scattering cross sections reduces to fitting a combination of two exponents for each harmonic of the profiles taken at different target thicknesses.

In experiments with the clearing field switched on, when the charged components of the beam are removed from the aperture,

$$J_0^k = A \exp(\pi (\bar{\sigma}_k^{00} - \bar{\sigma}_0^{00} - \bar{\sigma}_0^{01}) x)$$

where x is the target thickness. In this case

$$\ln(J_0^k(x)/J_0^0(x)) = \pi (\bar{\sigma}_k^{00} - \bar{\sigma}_0^{00}) x.$$

The spectrum of the scattering cross section without a charge-changing transformation of 11-keV H^0 on an Ar target, shown in Fig. 5, was obtained by fitting the straight lines to the values of $(\ln J_0^k/J_0^0)$, which were determined from the experimental profiles. The spectrum is also represented by a Gaussian curve which best approximates the distribution obtained. The corresponding scattering cross section is

$$\sigma(\theta) = \frac{0.1(\sigma^{10} + \sigma^{01})}{2\pi\theta_0^2} \exp(-\theta^2/2\theta_0^2)$$

with angle $\theta_0 = 3.6 \cdot 10^{-3}$ rad.

LITERATURE CITED

1. G. I. Dimov and O. Ya. Savchenko, "Increase in the intensity of beams of negative hydrogen ions and atoms from a pulsed ion source," *Zh. Tekh. Fiz.*, **38**, No. 11 (1968).
2. V. I. Batkin and V. N. Getmanov, "Analog-digital interface and on-line variation of the phase volume of a beam on an Élektronika-100I computer," *Prib. Tekh. Éksp.*, No. 5 (1983).
3. V. I. Batkin, V. N. Getmanov, O. Ya. Savchenko, and R. A. Khusainov, "Diagnostics of a plasma jet with grid electrodes," *Zh. Prikl. Mekh. Tekh. Fiz.*, No. 6 (1982).
4. V. I. Batkin, V. N. Getmanov, and O. Ya. Savchenko, "Increasing the brightness of the beam from an arc-discharge proton source," *Prib. Tekh. Éksp.*, No. 1 (1984).
5. V. I. Batkin, V. N. Getmanov, O. Ya. Savchenko, and R. A. Khusainov, "Effect of gas targets on the angular spread in a beam of fast hydrogen atoms," in: Abstracts of the 8th All-Union Conference on the Physics of Electron and Atomic Collisions [in Russian], Leningrad Institute of Nuclear Physics, Leningrad (1981).
6. S. K. Allison, "Experimental results on charge-changing collisions of hydrogen and helium atoms and ions at kinetic energies above 0.2 keV," *Rev. Mod. Phys.*, **30**, No. 4 (1958).
7. S. V. Starodubtsev and A. M. Romanov, *Passage of Charged Particles Through Matter* [in Russian], Izd. Akad. Nauk UzbSSR, Tashkent (1962).
8. N. V. Fedorenko, "Losses and capture of electrons by atoms, protons, and negative hydrogen ions in collisions with atoms and molecules. Experimental data on cross sections," *Zh. Tekh. Fiz.*, **40**, No. 12 (1970).
9. H. Tawara and A. Russek, "Charge-changing processes in hydrogen beams," *Rev. Mod. Phys.*, **45**, No. 2 (1973).
10. A. B. Wittkover and H. B. Gilbodi, "An experimental study of small angle scattering in charge-transfer collisions," *Proc. Phys. Soc.*, **90**, No. 2 (1967).
11. M. Abramowitz and I. A. Stegun (eds.), *Handbook of Mathematical Functions*, Dover, New York (1976).

GASDYNAMIC SELF-STRUCTURE UNDER UNSTABLE EVAPORATION
OF CATHODES IN A PULSED UNIPOLAR DISCHARGE

V. G. Zhogol', V. F. Reznichenko,
S. V. Selishchev, and A. A. Uglov

UDC 533.95

The action of concentration energy fluxes (pulsed discharge, laser radiation, electron beam, etc.) on a material is accompanied by instability of the erosion plasma-outflow [1-3]. The pulsations of the ionized gas near the target surface affect the thermophysical and gasdynamic processes, the nature of mass transfer and, hence, the physicomechanical properties of the action zone. In the general form there are erosion-plasma pulsations with two types of space-time structures: in the form of bundles [1, 3], i.e., intermittent plasma fluxes whose initial diameter is equal to that of the concentrated energy flux and jet pulsations [1, 2], i.e., individual plasma fluxes which arise at random and in different zones where the concentrated energy flux acts.

In this study we show that one more type of space-time structure of the erosion plasma, a helical structure, is observed when a pulsed unipolar discharge in a gaseous medium acts on cathodes made of different materials. We have found the conditions under which different types of erosion-flare structures are transformed into each other. We have demonstrated that the space-time evaporation structure depends on the pulse energy and length and on the form of the cathode material.